JOURNAL OF GEOPHYSICAL RESEARCH, VOL. 108, NO. D18, 4566, doi:10.1029/2002JD003369, 2003

Isotopic air sampling in a tallgrass prairie to partition net ecosystem CO_2 exchange

Chun-Ta Lai and Andrew J. Schauer
Department of Biology, University of Utah, Salt Lake City, Utah, USA

Clenton Owensby and Jay M. Ham
Department of Agronomy, Kansas State University, Manhattan, Kansas, USA

James R. Ehleringer
Department of Biology, University of Utah, Salt Lake City, Utah, USA

Received 31 December 2002; revised 16 May 2003; accepted 15 July 2003; published 16 September 2003.

[1] Stable isotope ratios of various ecosystem components and net ecosystem exchange (NEE) CO_2 fluxes were measured in a C_3-C_4 mixture tallgrass prairie near Manhattan, Kansas. The July 2002 study period was chosen because of contrasting soil moisture contents, which allowed us to address the effects of drought on photosynthetic CO_2 uptake and isotopic discrimination. Significantly higher NEE fluxes were observed for both daytime uptake and nighttime respiration during well-watered conditions when compared to a drought period. Given these differences, we investigated two carbon-flux partitioning questions: (1) What proportions of NEE were contributed by C_3 versus C_4 species? (2) What proportions of NEE fluxes resulted from canopy assimilation versus ecosystem respiration? To evaluate these questions, air samples were collected every 2 hours during daytime for 3 consecutive days at the same height as the eddy covariance system. These air samples were analyzed for both carbon isotope ratios and CO_2 concentrations to establish an empirical relationship for isoflux calculations. An automated air sampling system was used to collect nighttime air samples to estimate the carbon isotope ratios of ecosystem respiration (δ_R) at weekly intervals for the entire growing season. Models of C_3 and C_4 photosynthesis were employed to estimate bulk canopy intercellular CO_2 concentration in order to calculate photosynthetic discrimination against ^{13}C. Our isotope/NEE results showed that for this grassland, C_4 vegetation contributed ~80% of the NEE fluxes during the drought period and later ~100% of the NEE fluxes in response to an impulse of intense precipitation. For the entire growing season, the C_4 contribution ranged from ~68% early in the spring to nearly 100% in the late summer. Using an isotopic approach, the calculated partitioned respiratory fluxes were slightly greater than chamber-measured estimates during midday under well-watered conditions. In addition, time series analyses of our δ_R measurements revealed that occasionally during periods of high wind speed (increasing the sampling footprint) the C_3 cropland and forests surrounding the C_4 prairie could be detected and had an impact on the carbon isotopic signal. The implication is that isotopic air sampling of CO_2 can be useful as a tracer for evaluating the fetch of upwind airflow in a heterogeneous ecosystem. *INDEX TERMS:* 0315 Atmospheric Composition and Structure: Biosphere/atmosphere interactions; 1615 Global Change: Biogeochemical processes (4805); 1812 Hydrology: Drought; 3337 Meteorology and Atmospheric Dynamics: Numerical modeling and data assimilation; *KEYWORDS:* net ecosystem exchange, carbon isotopes, discrimination, isoflux, C_3-C_4 composition, photosynthesis model, canopy carbon modeling

Citation: Lai, C.-T., A. J. Schauer, C. Owensby, J. M. Ham, and J. R. Ehleringer, Isotopic air sampling in a tallgrass prairie to partition net ecosystem CO_2 exchange, *J. Geophys. Res.*, *108*(D18), 4566, doi:10.1029/2002JD003369, 2003.

1. Introduction

[2] Measurements of stable isotopes in atmospheric CO_2 have proven useful for distinguishing terrestrial and oceanic CO_2 uptake in global carbon cycles [*Keeling et al.*, 1979,

0148-0227/03/2002JD003369$09.00

1995; *Mook et al.*, 1983; *Tans et al.*, 1993; *Francey et al.*, 1995; *Ciais et al.*, 1995]. Differences in the extent of discrimination against ^{13}C between C_3 plants and the ocean provide the foundation for using $\delta^{13}C$ as a terrestrial tracer. This usage becomes more complex when considering terrestrial C_4 species because discrimination against ^{13}C by C_4 plants is similar to that of the ocean. Carbon isotopes have also proven quite useful for understanding the flux components of ecosystem-scale fluxes [*Flanagan and Ehleringer*, 1998; *Yakir and Sternberg*, 2000; *Bowling et al.*, 2001a]. At the ecosystem or regional terrestrial scales, we can capitalize on there being only two distinct photosynthetic and respiratory isotopic signals associated with fluxes between the biosphere and the atmosphere.

[3] The natural prairie grasslands of North America once consisted of both C_3 and C_4 grasses, but now few remnant prairie sites remain since much of the Great Plains region has been plowed for crop production. The Flint Hill tallgrass prairie in eastern Kansas remains as the largest pristine grassland ecosystem in North America [*Knapp and Seastadt.*, 1998], with C_3 versus C_4 dominance varying on a seasonal basis. Fire is the major factor that enhances or reduces the dominance of C_4 grasses [*Knapp and Medina*, 1999], but this information alone provides no insight into seasonal productivity, respiration, and decomposition of C_3 and C_4 grass components of the prairie. The interplay among water availability, nitrogen content, and grazing activities makes C_4 dominance less predictable. For instance, drought may negatively impact the mortality of invading C_3 species, but it also inhibits C_4 grass activities because of their shallower rooting depth [*Axmann and Knapp*, 1993]. Therefore the proportions of C_3 versus C_4 contributions to the net ecosystem exchange (NEE) CO_2 fluxes in this prairie ecosystem could change in response to precipitation pulses at different times of the growing season.

[4] Because of the biochemical differences between C_3 and C_4 plants, C_4 photosynthesis discriminates less against ^{13}C than C_3 photosynthesis. On average, the carbon isotope ratios of C_3 and C_4 plants are -12 and -28‰, respectively [*Farquhar et al.*, 1989]. This difference in the carbon isotope ratios of C_3 and C_4 species imprints an isotopic signal to the atmosphere that can be utilized to separate their relative contributions to overall CO_2 fluxes.

[5] Eddy covariance measurements for C_4-dominated tallgrass prairie have been published [*Verma et al.*, 1992; *Kim et al.*, 1992; *Ham and Knapp*, 1998; *Suyker and Verma*, 2001], but quantifying one-way gross fluxes and the C_3/C_4 contributions to these fluxes has remained unconstrained. In addition, nighttime fluxes have been difficult to measure due to weakly turbulent mixing associated with atmospheric stratification and/or drainage flow, leading to potential underestimation of respiratory fluxes [*Goulden et al.*, 1996; *Lavigne et al.*, 1997]. Alternative methods for estimating the nighttime fluxes to assess annual carbon budget have been described by *Lai et al.* [2002a]. Here stable isotopes are an additional powerful tool for partitioning NEE flux components [*Yakir and Sternberg*, 2000].

[6] Carbon exchange processes between the biosphere and the atmosphere manipulate $\delta^{13}C$ abundance of the atmospheric CO_2, giving enriched ^{13}C signals during photosynthesis and adding a ^{13}C-depleted signal when respiration dominates [*Farquhar et al.*, 1989; *Flanagan and Ehleringer*, 1998]. These distinct ^{13}C signatures are useful tracers to characterize gross fluxes [*Yakir and Wang*, 1996]. Canopy biophysical models can be used to predict the within-canopy transport, source density distributions, and carbon isotope ratios of CO_2 [*Raupach*, 2001; *Baldocchi and Bowling*, 2003]. *Bowling et al.* [1999, 2001a] developed field techniques to estimate isoflux, allowing for partitioning NEE into photosynthesis and respiration with ^{13}C measurements. However, an isotopic partitioning approach has never been applied to a heterogeneous vegetation ecosystem where the isotopic imbalance between photosynthesis and respiration is unknown. Such a task should be largely dependent on our ability to quantify the $^{13}C/^{12}C$ abundances of each exchange process.

[7] The objectives of this study are threefold: (1) to partition relative contributions of C_3 and C_4 composition to the net carbon exchange over a period with contrasting soil moisture contents, (2) to partition net ecosystem CO_2 exchange fluxes into their photosynthetic and respiratory components in a C_3-C_4 mixture grassland, and (3) to monitor the natural variations in the carbon isotope ratios of ecosystem respiration at weekly intervals and investigate possible causes for such variability. To accomplish this, air, plant, and soil samples were measured for both carbon isotope ratios and CO_2 concentrations in conjunction with simultaneous eddy covariance measurements. Nighttime air samples were collected weekly to estimate the $\delta^{13}C$ of ecosystem respiration (δ_R). This data set is unique for its relatively high frequency of δ_R measurements at a C_3-C_4 prairie and provides a great opportunity to explore the dynamics associated with isotopic variation in an ecosystem with heterogeneous vegetation types.

2. Method

[8] Conservation of mass is the fundamental principle to describe scalar transport through canopy-atmosphere interface. *Yakir and Wang* [1996] derived isotopic mass balance equations for $\delta^{13}C$ to partition net ecosystem exchange fluxes over grassland. *Bowling et al.* [2001a] capitalized on Yakir and Wang's work and further developed a more generalized formulation to extend such applications to include forest canopies. Here we briefly review the mass balance equations for $^{12}CO_2$ and $^{13}CO_2$ fluxes for combining isotope with eddy covariance measurements in order to partition NEE. *Bowling et al.* [2003] have recently made an effort to standardize the notations for isoflux and net ecosystem exchange of $^{13}CO_2$.

2.1. Mass Balance for $^{12}CO_2$ and $^{13}CO_2$ Fluxes

[9] Considering the scalar CO_2, the net exchange fluxes across an arbitrary plane over a plant canopy represent the balance of two contrary processes, photosynthesis (F_A) and respiration (F_R). Therefore

$$\mathrm{NEE} = F_R + F_A. \tag{1}$$

[10] The sign convention is upward flux positive so that $F_A < 0$ and $F_R > 0$. We note that the storage flux term is small for a grassland which typically has high wind speeds. Each of the processes in equation (1) is associated with an isotopic signature. When written in δ notation ($\delta = (R/R_{\mathrm{std}} - 1) \cdot 1000$,

where R and R_{std} are the isotope ratios of the scalar and a known standard, respectively), an isotopic mass balance equation can be given by

$$\delta_N \times \mathrm{NEE} = \delta_R F_R + \delta_p F_A, \tag{2}$$

where δ_N represents the isotopic composition of the CO_2 exchanged across an arbitrary surface (where eddy covariance fluxes were measured), δ_R is the isotopic composition of ecosystem respired CO_2, and δ_p is the isotopic composition of the CO_2 fixed via photosynthesis. With NEE measured by the eddy covariance system, equations (1) and (2) provide two required equations to solve for two unknowns in F_A and F_R, if δ_N, δ_R, and δ_p can be measured or modeled. We discuss methods to estimate these isotopic signatures next.

2.1.1. Estimate of δ_N

[11] Rearranging equations (1) and (2), we can see that

$$\begin{aligned} F_A &= \frac{\delta_N - \delta_R}{\delta_p - \delta_R}\mathrm{NEE} \\ F_R &= \frac{\delta_p - \delta_N}{\delta_p - \delta_R}\mathrm{NEE} \end{aligned} \tag{3}$$

in analogy to the relationship developed by *Yakir and Wang* [1996]. They characterized δ_N, δ_R, and δ_p by measuring isotopic compositions of plant and soil organic materials, which typically represent long-term (months to years) integrated isotopic values. To quantify the dynamics of carbon exchange between the atmosphere and vegetation canopies at shorter timescales (from seconds to hours), *Bowling et al.* [1999, 2001a] explored several field techniques to estimate δ_N, δ_R, and δ_p. Here we follow the method of *Bowling et al.* [2001a] to characterize δ_N and δ_R but using a different approach to estimate δ_p. Readers who are interested in the derivation of equations (4) and (5) are encouraged to see the work of *Bowling et al.* [2001a, 2003].

[12] According to *Bowling et al.* [2001a], the eddy isoflux ($F_\delta = \delta_N \times$ NEE) can be approximated using 30-min mean CO_2 concentration measurements ($\bar{C}$) via

$$\begin{aligned} F_\delta &= \left(2m\overline{C} + b\right)\rho\overline{w'C'} + m\rho\overline{w'C'C'} \\ &\approx \left(2m\overline{C} + b\right)\rho\overline{w'C'}, \end{aligned} \tag{4}$$

where the higher-order term is small and can be neglected, ρ is the air density (mol m^{-3}), w is the vertical wind speed (m s^{-1}), C is CO_2 concentration, and overbar indicates time averaging; m and b are regression coefficients from an empirical relationship between CO_2 concentration and $\delta^{13}C$ of CO_2 in flasked air ($\delta^{13}C_a$):

$$\delta^{13}C_a = m \cdot C + b. \tag{5}$$

Given a set of flasks, m and b can be obtained by performing a linear regression for C versus $\delta^{13}C_a$. From equations (4) and (5) we can estimate $\delta_N (= 2m\bar{C} + b)$ by collecting air samples during the day. *Bowling et al.* [2001a] empirically demonstrated that this method was robust for air samples collected across orders of timescales. We reiterate that equation (4) was derived based on the assumption that an empirical relationship exists between daytime $\delta^{13}C$ and CO_2 concentration (i.e., equation (5)). The present study represents a worst case scenario for such relationship because of the large differences in carbon isotope discrimination between C_3 and C_4 species.

2.1.2. Estimate of δ_R

[13] A two-end mixing model, the so-called "Keeling plot" approach, can be used to estimate the isotopic composition of respired CO_2 (δ_R) [*Keeling*, 1958]. Keeling plots were constructed by plotting the inverse of CO_2 mole fraction against corresponding $\delta^{13}C$ ratio for a set of flasks (typically 10–15 samples), given by

$$\delta^{13}C_a = \frac{\mathrm{slope}}{C} + \delta_R. \tag{6}$$

[14] The geometric mean (Model II) regression was used for each Keeling plot in order to account for measurement errors on both dependent and independent variables [*Sokal and Rohlf*, 1995; *Flanagan et al.*, 1996]. The assumption behind the Keeling approach is that the respired CO_2 fluxes are proportionally uniform for every component of an ecosystem so that one representative flux-weighted isotopic composition exists. Outliers were removed before constructing each Keeling plot following the procedure described by *Bowling et al.* [2002].

2.1.3. Estimate of δ_p

[15] The $\delta^{13}C$ of assimilated carbon (δ_p) during photosynthesis can be calculated approximately [*Bowling et al.*, 2001a], by

$$\delta_p \approx \delta_a - \Delta, \tag{7}$$

where δ_a is the carbon isotopic composition of background CO_2 (approximately −8‰) and Δ is the discrimination against ^{13}C during photosynthesis. *Bowling et al.* [2001a] used an aerodynamic approach in coupling with a Fick's law to estimate canopy conductance and the bulk canopy intercellular CO_2 concentration (C_i), and then calculate Δ using [*Farquhar et al.*, 1989; *Farquhar and Lloyd*, 1993]

$$\Delta = a + (b_x - a)\frac{C_i}{C_a}, \tag{8}$$

where a is the diffusional fractionation (4.4‰), b_x is the enzymatic fractionation (~27.5 and 0.6 for C_3 and C_4 plants, respectively), and C_a is the CO_2 concentration of ambient air.

[16] The extent of discrimination against ^{13}C during photosynthesis is greater for C_3 than C_4 species [*Lloyd and Farquhar*, 1994]. Therefore canopy-scale discrimination (Δ_E) should be flux-weighted according to relative productivity of the C_3 and C_4 plants as

$$\Delta_E = \frac{\sum_{i=3\,\mathrm{or}\,4} A_i\Delta_i}{\sum_{i=3\,\mathrm{or}\,4} A_i}, \tag{9}$$

where index $i = 3$ represents C_3 species and $i = 4$ represents C_4 species.

Table 1. Physiological Parameters Used in the C_3 and C_4 Photosynthesis Models[a]

Parameters	C_3	C_4	Units	References
Initial slope of photosynthetic CO_2 response	...	0.7	mol m^{-2} s^{-1}	*Collatz et al.* [1992]
Maximum Rubisco capacity, V_{cmax} at 25°C	120	30	μmol m^{-2} s^{-1}	*Colello et al.* [1998]
Quantum yield	0.08	0.067	mol mol^{-1}	*Campbell and Norman* [1998] and *Collatz et al.* [1992]
Leaf absorptivity	0.8	0.8		*Campbell and Norman* [1998]
Stomatal slope factor, m_s	9	4		*Sellers et al.* [1996]
Stomatal intercept factor, b_s	0.01	0.04		*Sellers et al.* [1996]
Leaf clumping factor, λ	0.95	0.95		*Sellers et al.* [1996]
f_d	0.015	0.025		*Sellers et al.* [1996]

[a]Details on the mathematical expressions and parameter descriptions are given by *Farquhar et al.* [1980] for C_3 photosynthesis and *Collatz et al.* [1992] for C_4 photosynthesis. Dark respiration $R_d = f_d V_m$ was modeled as a function of Rubisco capacity (V_m).

[17] *Bowling et al.* [2001a] noted that the estimate of Δ is very sensitive to the estimate of canopy conductance using the aerodynamic approach, consequently the partitioning results of NEE. For the present study, we employed a different approach by directly modeling the dynamics of C_i/C_a ratio using two photosynthesis models, one for C_3 and the other for C_4 plants. Below, we briefly described this modeling framework and the physiological parameters needed for the model.

2.2. Modeling Canopy Assimilation and Conductance

[18] To estimate bulk canopy assimilation for a C_3-C_4 mixture grassland, both photosynthetic pathways needed to be considered independently. The total assimilation rate is the sum of C_3 and C_4 photosynthetic fluxes. The bulk canopy conductance and intercellular CO_2 concentration should be flux-weighted, based on the relative contributions of C_3 and C_4 species. In modeling interactions between leaf assimilation and stomatal conductance, we used the C_3 photosynthesis model of *Farquhar et al.* [1980] and the simplified C_4 photosynthesis model of *Collatz et al.* [1992] coupled with a stomatal conductance model developed by *Ball et al.* [1987]. Following Farquhar et al., net photosynthesis (A_n) for C_3 species can be modeled by three rate-limiting steps

$$A_n \approx \min\left\{\begin{matrix} J_E(Q_p, T_l) \\ J_C(V_m, T_l) \\ J_S \end{matrix}\right\} - R_d(V_m, T_l), \tag{10}$$

where min{} represents "the minimum of", J_E, J_C, and J_S are the assimilation rates limited by light, ribulose bisphosphate (R_uBP) carboxylase (or Rubisco), and the export rate of synthesized sucrose, respectively, R_d is the dark respiration rate, Q_p is the photosynthetic photon flux density, T_l is the leaf surface temperature, and V_m is the Rubisco capacity adjusted by soil moisture content and leaf temperature.

[19] In the case of C_4 photosynthesis, *Collatz et al.* [1992] proposed a simplified C_4 model that can be expressed in the same form as equation (10), with J_E and J_C still referring to limits by light intensity and Rubisco capacity, and J_S now refers to a phosphoenolpyruvate (PEP)-carboxylase limitation. The advantage of this simplified model is that with a smaller number of adjustable parameters, it is more easily implemented into a more complex modeling framework to predict photosynthesis at the canopy scale. For further details about parameter description in the photosynthesis models, see the work of *Farquhar et al.* [1980] and *Collatz et al.* [1992].

2.2.1. Stomatal Conductance Model

[20] The coupling between photosynthesis and stomatal conductance can be achieved by linking the photosynthesis model to a stomatal conductance model [*Ball et al.*, 1987; *Collatz et al.*, 1992], given by

$$g_s = \frac{m_s \cdot A_n \cdot \mathrm{RH}}{C_s} + b_s, \tag{11}$$

where m_s and b_s are species-specific parameters (determined by gas-exchange measurements), C_s is the CO_2 concentration at the leaf surface, and RH is the relative humidity. Different values of m_s and b_s for C_3 and C_4 species are given in Table 1.

[21] A leaf energy budget was used and solved iteratively with the photosynthesis-stomatal conductance module in order to estimate T_l; iteration continued until the difference in leaf surface temperatures between two consecutive runs was less than 10^{-5}°C. The physiological parameters required to drive the C_4 photosynthesis model were measured during the First International Satellite Land Surface Climatology Project (ISLSCP) Field Experiment (FIFE) [*Sellers et al.*, 1996; *Colello et al.*, 1998]. Other required physiological inputs were derived from the existing literature [*Collatz et al.*, 1992; *Chen et al.*, 1994; *Campbell and Norman*, 1998; *Lai et al.*, 2000, 2002b]. Table 1 summarizes the physiological parameters used in the photosynthesis models.

2.2.2. Drought Effects

[22] Previous research showed that changes in available soil water strongly modulated CO_2 fluxes at this grassland because of the physiological stresses imposed under drought [*Kim and Verma*, 1991]. Here we incorporated a drought effect on carbon uptake in the photosynthesis models following the observations of *Colello et al.* [1998], in which an empirical water stress function was developed to adjust Rubisco capacity as

$$\begin{aligned} V_m &= f_w(\theta) V_{c\max} \\ f_w &= \frac{\theta - \theta_w}{\theta_i - \theta_w}, \end{aligned} \tag{12}$$

where θ is the mean surface soil moisture content, θ_w and θ_i are the soil moisture contents at wilting point and at the onset of water stress, and V_{cmax} is the maximum Rubisco

capacity under nonstress conditions. For this study, we used values of $\theta_w = 0.1$ and $\theta_i = 0.16$, values that were at the lower end of those reported by *Colello et al.* [1998, Figure 8]. We reiterate that equations (10)–(12) should be considered separately for both C_3 and C_4 photosynthesis through the parameterization shown in Table 1.

2.2.3. Scaling From Leaf to Canopy Level

[23] In order to scale leaf-level calculations of photosynthetic discrimination to the canopy level we need an estimate of the effective bulk canopy C_i/C_a. One of the scaling approaches is to express the physical and physiological properties of the canopy at different depths as a function of those at the canopy top. This is done in order to simplify model complexity so that such biospheric models can be easily implemented in the regional-scale General Circulation Model (GCM) models and because field observations support the hypothesis that physiological properties (e.g., leaf nitrogen content and thus $V_{c\max}$) within the canopy are distributed according to light attenuation [*Sellers*, 1985; *Hirose and Werger*, 1987; *Field*, 1991; *Leuning et al.*, 1995]. Since most of the available meteorological measurements are collected above the canopy, it is plausible adopting this scaling approach. According to *Sellers et al.* [1996], a scaling factor (Π) can be defined such that

$$A = A_0\Pi$$
$$\Pi = \frac{\lambda\nu\left(1-e^{-\bar{k}L_T/\lambda}\right)}{\bar{k}}, \tag{13}$$

where A is the canopy photosynthesis, A_0 is the net photosynthesis for the leaves at the top of the canopy, λ is the clumping factor, ν is canopy greenness fraction, L_T is the leaf area index (LAI) (separately for C_3 and C_4 species), and $\bar{k}$ is the mean canopy extinction coefficient, which was weighted by daily mean radiation and assumes that the canopy has a spherical leaf angle [*Campbell and Norman*, 1998]. The diurnal Sun zenith angle was calculated according to the formulation by *Campbell and Norman* [1998].

[24] Leaf-level assimilation rate was scaled to the canopy level separately for C_3 and C_4 species. The canopy assimilation was then used to calculate bulk canopy conductances (G_c) using equation (11). Finally, bulk intercellular CO_2 concentration can be estimated as

$$C_i = C_a - \frac{1.6A}{G_c}. \tag{14}$$

2.3. Soil Respiration

[25] To incorporate soil CO_2 flux into our model, we adopted an empirical equation based on chamber measurements as functions of soil temperature and moisture content [*Mielnick and Dugas*, 2000], which is given by

$$R_{\text{soil}}(\theta, T_s) = 6.42e^{0.087T_s}\left[2.12(\theta - 0.1)(0.7 - \theta)^{1.46}\right], \tag{15}$$

where R_{soil} is the rate of soil respiration (g C m^{-2} d^{-1}) and T_s is soil temperature (°C). This function was tested against measurements collected at the Konza Prairie and explained 76% of the observed flux variability [*Mielnick and Dugas*, 2000].

3. Field Experiment

3.1. Study Site

[26] This research was conducted on the Rannells Flint Hills Prairie Preserve near Manhattan, Kansas (39°12′N, 96°35′W, 324 m above sea level), which is the largest unplowed tract of tallgrass prairie in North America. The vegetation was a mixture of C_3 and C_4 grass species. The C_4 warm-season grasses included *Andropogon gerardii* Vitman (Big bluestem), *Sorghastrum nutans* (L.) Nash. (Indiangrass), and *Andropogon scoparius* Michx. (Little bluestem). The C_3 grass species included *Carex* Sp. (Sedge) and *Amphiachyris dracunculoides* (DC.) Nutt. ex Rydb. (annual broomweed). Soils at the site were characterized as silty clay loams. The 30-year average annual precipitation is 840 mm, with roughly 60% occurring in the spring and early summer. The site has been burned annually (typically in the last 10 days of April) and has not been grazed since 1997. The mean canopy height (h) was 0.45 m at the time of study.

[27] A 20-day period in July 2002 was selected to address the effects of drought on net ecosystem exchange fluxes. Previous studies have shown that soil water availability has a profound impact on NEE at this site [*Kim and Verma*, 1991; *Steward and Verma*, 1992; *Colello et al.*, 1998]. The site had received only 15 mm of rain since the beginning of growing season and was experiencing a severe drought until an intense rain event (87 mm) occurred on 28 July (day of year, DOY 209, Figure 1). The mean surface soil moisture contents were 0.14 and 0.41 m^3 m^{-3} and LAI was 1.8 and 2.1 for the dry and wet periods, respectively.

3.2. Canopy Mass and Energy Exchange

[28] The turbulent fluxes of momentum, sensible heat, latent heat, and CO_2 above the grass canopy were measured with an open-path eddy covariance system consisting of a CO_2/H_2O gas analyzer (LI-7500, LI-Cor Inc., Lincoln, Nebraska) and a triaxial sonic anemometer (CAST3, Campbell Scientific Inc., Logan, Utah). Sensor separation was approximately 0.1 m, and the LI-7500 sensor head was tilted 15° to the north to minimize the direct beam radiation effect on the gas analyzer (LI-7500 Field Note 1, Li-Cor, 2002). The system was mounted on a mast at 3 m above ground (~6 times of canopy height) and the signals were sampled at 10 Hz with a CR23X data logger (Campbell Scientific). Post data processing included coordinate rotation and density corrections on CO_2 and water vapor fluxes [*Webb et al.*, 1980]. Details on the signal processing are given by *Ham and Heilman* [2003].

3.3. Other Environmental Variables

[29] In addition to the eddy flux measurements, ancillary meteorological and hydrological variables were also measured. Net radiation was measured with a net radiometer (Q7.1, Radiation Energy Balance Systems, Seattle, Washington) approximately 1.8 m above ground. Photosynthetically active radiation (PAR) was measured using a quantum sensor (LI-190SA, LI-Cor). Precipitation was measured with a tipping-bucket rain gauge. A Ta/RH probe (HMP45C, Campbell Scientific) was used to measure mean air temperature and relative humidity. Soil heat flux and soil temperature were measured using heat flux plates (HFT-3, Radiation Energy Balance Systems) at 0.05 m and dual probe heat capacity sensors at 0.025 m [*Campbell et al.*,

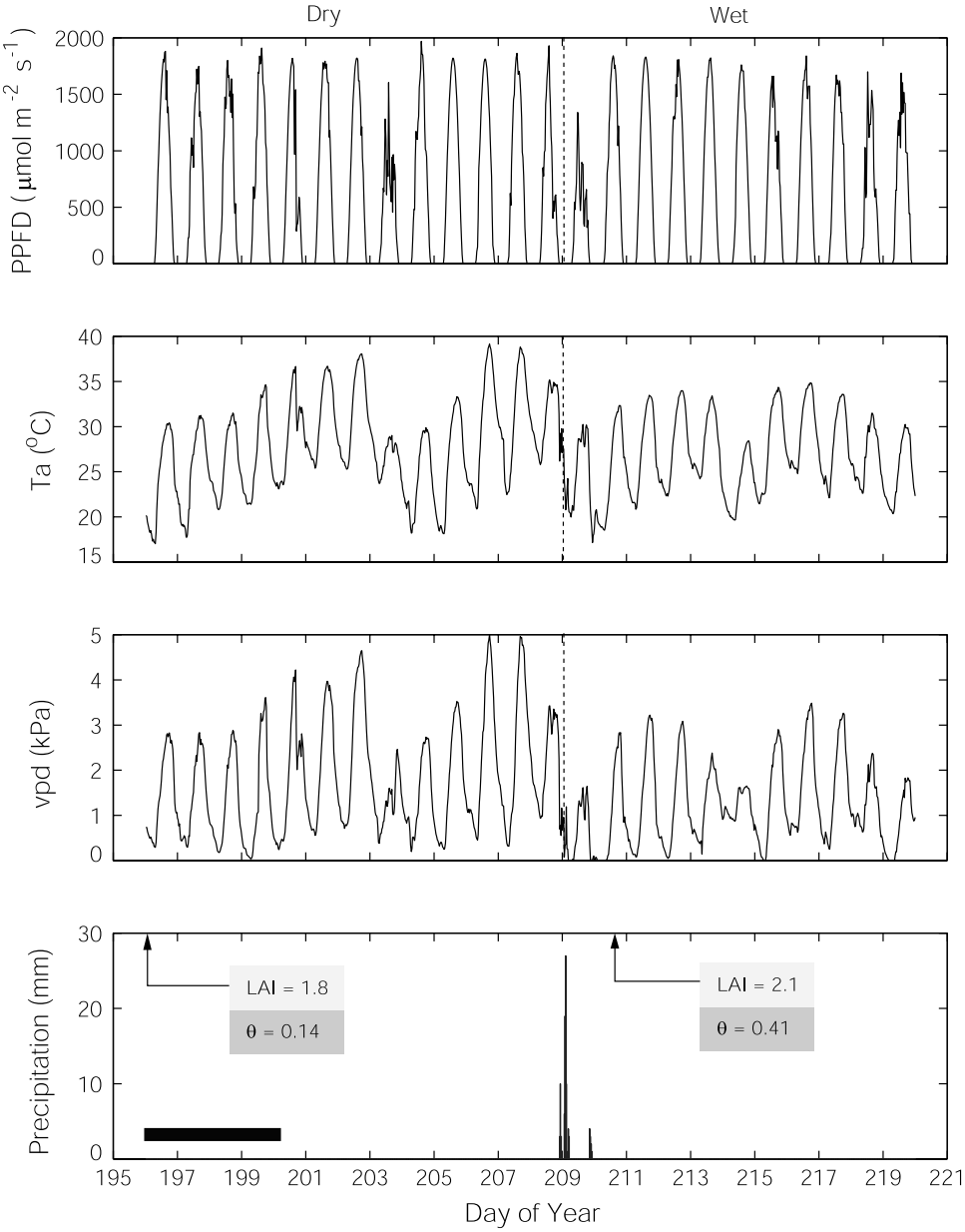

Figure 1. Meteorological conditions of the study period. Diurnal patterns of photosynthetic photon flux density (PPFD), mean air temperature (T_a), vapor pressure deficit (vpd), and precipitation are shown. Leaf area index (LAI, $m^2\ m^{-2}$) and mean surface soil moisture content (θ, $m^3\ m^{-3}$) measured on DOY 196 and 210 are also shown. The thick bar indicates the period of our intensive isotope field campaign.

1991]. All these sensors were sampled every 10 s using a CR23X data logger. Soil moisture contents were measured daily at 0600 local standard time (LST) using dual probe heat capacity sensors (two sensors at 0.025 m and one sensor at 0.1 m) in an automated fashion [*Tarara and Ham*, 1997]. Soil moisture also was measured periodically by collecting gravimetric samples. Typically, three soil cores were collected between 0 and 0.15 m to calibrate heat capacity sensors.

3.4. Stable Isotope Measurements

3.4.1. Carbon Isotope Ratio of Ecosystem Respiration

[30] Starting in March 2002, an automated air-flask sampling system (sampler) was deployed to collect air samples weekly for $\delta^{13}C$ analyses in atmospheric CO_2. The sampler system was designed and built for unattended collection of 15 flasks, made possible using a 16-position rotary valve (EMTST16MWM, Valco Instruments Company, Inc., Houston, Texas) controlled by a CR23X data logger. A detailed description of the automated sampling system is given by *Schauer et al.* [2003].

[31] Using the automated sampler, nighttime air samples were collected at two heights inside the canopy ($0.1h$ and $0.8h$) at specified CO_2 concentrations in order to obtain sufficient statistical confidence when constructing the Keeling plot [*Pataki et al.*, 2003]. Air samples were dried with magnesium perchlorate during collection and stored in 100-ml glass flasks with Teflon stopcocks (Kontes Glass

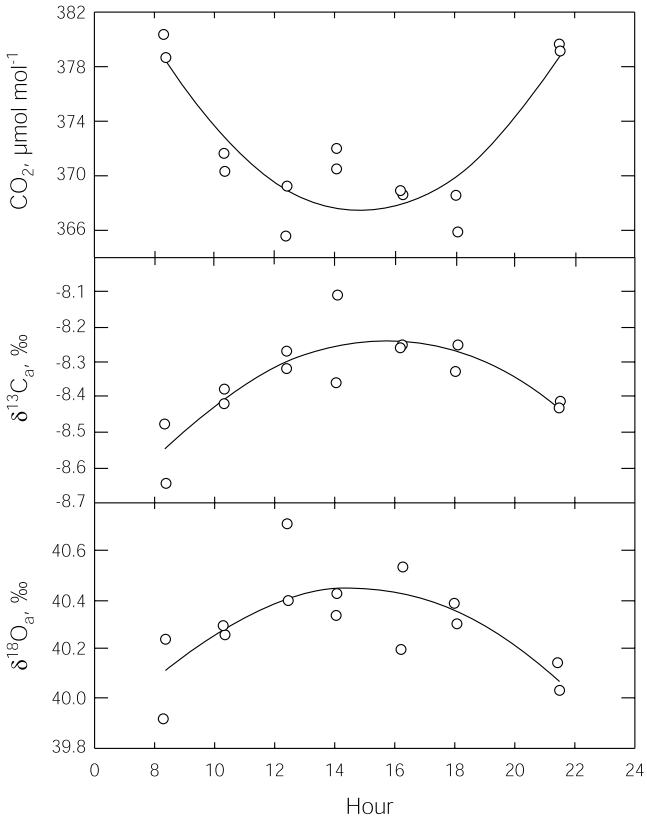

Figure 2. Diurnal variations of measured CO_2 concentration and $\delta^{13}C$ and $\delta^{18}O$ of atmospheric CO_2 on 17 July 2002. Two flasks are collected at 0.8*h* at each sampling session, where *h* is the canopy height. Here $\delta^{18}O_a$ is in standard mean ocean water (SMOW) scale.

Co., Vineland, New Jersey). Flasks were collected by a field assistant and shipped back to Stable Isotope Ratio Facility For Environmental Research at the University of Utah for analyses. Carbon isotope ratios of CO_2 in the flasks were measured on a continuous-flow isotope ratio mass spectrometer (Finnigan MAT 252, San Jose, CA) as described by *Ehleringer and Cook* [1998]. CO_2 was separated from N_2O by gas chromatography and corrections for the presence of ^{17}O were applied. Long-term precision of the $\delta^{13}C$ measurements using the approach described by *Ehleringer and Cook* [1998] was 0.12‰. The $\delta^{13}C$ values are reported relative to the Vienna Peedee Belemnite (VPDB) standard. The CO_2 concentration within each flask was measured in the laboratory to a precision of 0.3 ppm following the method of *Bowling et al.* [2001b].

3.4.2. Intensive Isotope Measurements

[32] In additional to the weekly sampling of carbon isotope ratio of ecosystem respiration, intensive field campaigns were carried out to measure $\delta^{13}C$ values of different ecosystem components. The carbon isotope ratios of leaves, litter, fine roots, and soil organic matter were measured in July 2002. Five replicate samples were collected for analyses, including five separate soil pits. All organic samples were oven-dried at 70°C immediately after collection. The carbonate content in the soils at this site was low and acid washing had only a minimal impact on the $\delta^{13}C$ value (0.1‰ between acid-washed and nontreated samples). Organic samples were ground to fit through a No. 20 mesh, and 2- or 10-mg subsamples (for plant and soil samples, respectively) were combusted and analyzed on a mass spectrometer (Finnigan delta S operated in a continuous-flow mode). The long-term precision for $\delta^{13}C$ measurements of organic samples was 0.2‰.

[33] Daytime air samples were manually collected every 2 hours between 0800 and 2000 hours for 3 consecutive days beginning in the afternoon of 16 July 2002. These air samples were collected from three heights above the canopy, dried by flowing through magnesium perchlorate trap before being stored in 100-ml glass flasks. In total, 60 daytime flasks were collected during the field campaign in July.

4. Results

4.1. Diurnal Patters of NEE

[34] Figure 1 shows the environmental conditions for our study period. Although the photon flux intensity was about the same for clear days between the dry and the wet period, mean air temperature (T_a) and vapor pressure deficit (vpd) were notably higher during drought, which created a much stronger atmospheric evaporative demand. The contrasting soil moisture contents of the two periods not only strongly influenced the canopy physiology but also had an impact on soil CO_2 fluxes. The drought severely suppressed carbon assimilation of grasses during midday (described below). As a result, only small diurnal variations in CO_2 concentration, $\delta^{13}C$ and $\delta^{18}O$ of atmospheric CO_2 were detected (Figure 2) on 17 July 2002 (DOY 198). While we observed much greater isotopic variations under wetter conditions, these small but detectable carbon isotope ratio differences in atmospheric CO_2 were still sufficient for evaluating gross CO_2 fluxes.

[35] Figure 3 shows the comparison of the diurnal NEE patterns from the eddy covariance measurements between the two periods. Midday canopy carbon uptake rates were much stronger under well-watered conditions; however, significantly higher respiratory fluxes were also observed for the same period. The rapid recovery of the soil CO_2 efflux suggested a significant increase in both microbial and root respiration activities. Interesting NEE patterns were noted during the dry period. In general, biological flux

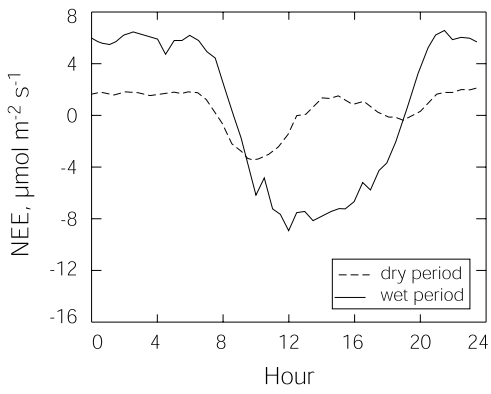

Figure 3. Comparison of diurnal patterns for the net ecosystem CO_2 exchange (NEE) measurements between the drought and the well-watered periods. The NEE values represent the mean values averaged over a 10-day period.

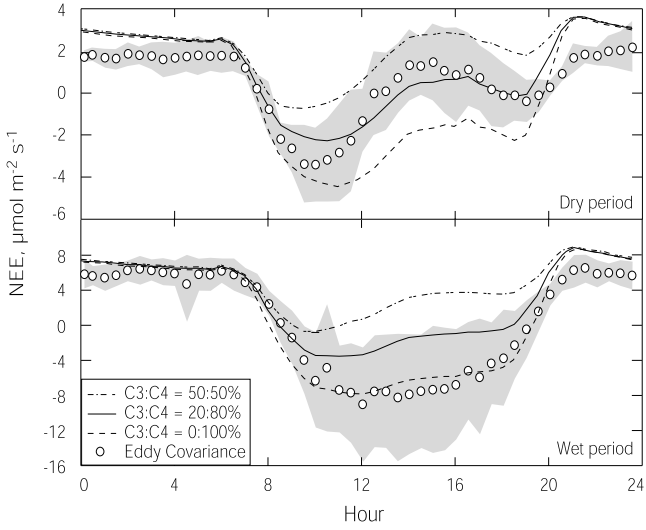

Figure 4. Comparison between modeled and measured NEE CO_2 fluxes for the two study periods, each averaged over a 10-day period. Measurements of NEE CO_2 fluxes are shown with one standard deviation around mean in gray. Modeled NEE values were calculated with three scenarios of C_3-C_4 contributions to primary productivity: C_4 = 50, 80, and 100%, respectively.

activities within the ecosystem were low (NEE nearly equals to zero for both daytime and nighttime). Most of the carbon gain occurred in the early morning hours when T_a and vpd were mild. The NEE values switched sign from negative to positive in the afternoon, indicating a net carbon loss from this ecosystem during these daylight periods. Photosynthetic activities recovered somewhat by late afternoon when temperatures had cooled, but this was apparently insufficient to increase photosynthetic rates enough to offset respiration rates.

[36] The observed dissimilarity of the diurnal NEE patterns between drought and well-watered conditions raised two partitioning questions: (1) What proportions of NEE fluxes was contributed by C_3 versus C_4 species? (2) What proportions of NEE fluxes resulted from canopy assimilation versus ecosystem respiration? To evaluate both questions, we employed two photosynthesis models, one for C_3 and the other for C_4 species coupled with a stomatal conductance model. This modeling approach was adopted to first estimate the relative productivity of C_3 and C_4 grasses and intercellular CO_2 concentration (C_i). The canopy photosynthetic discrimination against ^{13}C was modeled using equation (8) for C_3 and C_4 species and then weighted by their relative productivities as described by equation (9).

4.2. Partitioning C_3/C_4 Contributions to NEE

[37] The modeled proportion of C_3 and C_4 contribution to NEE is shown in Figure 4. We ran our model with three scenarios considering different C_3-C_4 proportions, i.e., C_4 contributing 50, 80, and 100% for the two periods. During the dry period, modeled NEE values showed the closest agreement with the observations when C_4 photosynthesis contributed 80% to overall NEE values. Overall, the model captured the diurnal patterns of measured NEE reasonably well, particularly during daytime hours when substantial NEE fluctuations were observed (see also Table 2). Some small differences between predicted and observed NEE values were observed during the nighttime period. A large portion of these nighttime differences may be attributable to the disagreement between measurement techniques, i.e., eddy covariance versus chamber measurements. The latter was used in our model to describe soil respiration. For the wet period, modeled and measured NEE values had the closest agreement when C_4 photosynthesis contribution to overall NEE reached 100% (also see Table 2). The model underestimated NEE fluxes when higher C_3 percentages were considered. This was due to a lower predicted maximal C_3 photosynthetic rate at light saturation.

[38] We further evaluated our model and the predicted C_3/C_4 contributions to NEE using our carbon isotope measurements. The distinction in the carbon isotope fractionation between C_3 and C_4 species provided a significantly different isotope signal to their relative photosynthetic fluxes. While there are photosynthetic-based carbon isotope differences in the fluxes during CO_2 uptake, there is apparently no fractionation during respiration [*Lin and Ehleringer*, 1997]. The $\delta^{13}C$ values of organic matter contributing to respired CO_2 should therefore be roughly similar. A two-source mixing model can be used to calculate C_4 fraction to NEE (f) by

$$\delta_R = f\delta^{13}C_4 + (1-f)\delta^{13}C_3, \tag{16}$$

where $\delta^{13}C_3 = -27.9$ (±0.54 SE)‰ and $\delta^{13}C_4 = -12.3$ (±0.19 SE)‰ are measured carbon isotope ratios of plant organic matter for C_3 and C_4 species, respectively. Nighttime air samples collected by the automated sampler were used to construct Keeling plots as shown in Figure 5. The δ_R values were estimated to be −15.0 (±0.29 SE)‰ during the dry period and −12.1 (±0.56 SE)‰ during the wet period. Using an isotope mass balance approach, the C_4 fraction to NEE was calculated to be 82% during drought period and 100% during well-watered periods. This result independently confirmed our model calculation for the proportion of the C_3/C_4 contribution to the NEE fluxes.

[39] Perhaps differences in the rooting depths between C_3 forbs and C_4 grasses and responsiveness to soil moisture changes can explain the shift in C_3 versus C_4 contributions to NEE before and after the rain. *Knapp* [1986] and *Knapp and Medina* [1999] showed similar leaf water potentials in the C_4 grasses compared to C_3 forbs under wet conditions, but significantly lower leaf water potentials in C_4 grasses under a drought period. A greater portion of effective root biomass was observed at depth for C_3 forbs during drought [*Weaver*, 1958]. While photosynthetic rates in C_4 grasses

Table 2. Regression Statistics for the Comparison Between Modeled and Measured NEEs for Both Dry and Wet Periods[a]

Period	Modeled C_4%	A	B	R^2	RMSE
Dry	80	0.79	−0.31	0.82	0.95
Wet	100	0.89	−0.32	0.95	1.50

[a]The linear regression model is $y = Ax + B$, where y and x are measured and modeled variables, respectively. The statistical variables A and B represent the regression slope and intercept, respectively. The coefficient of determination (R^2) and the root-mean-square error (RMSE, μmol m^{-2} s^{-1}) are also shown.

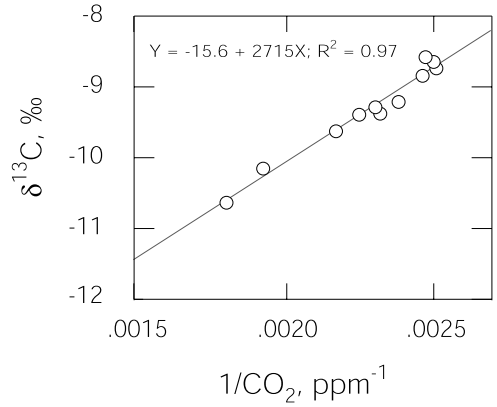

Figure 5. An example of the Keeling plot. Nighttime air samples were collected by the sampler on DOY 209 to estimate $\delta^{13}C$ of ecosystem respired CO_2 for the dry period.

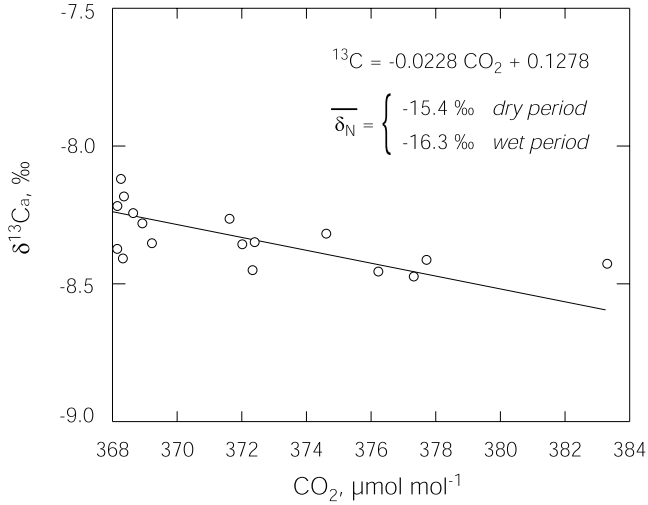

Figure 6. Relationship between $\delta^{13}C$ and CO_2 concentration of daytime atmospheric CO_2. A linear relationship $\delta^{13}C_a = m \cdot C + b$ was obtained with $m = -0.0228$ (±0.0051 SE) and $b = 0.1278$ (±1.9078 SE). The mean isotopic composition of the CO_2 associated with NEE exchange $\overline{\delta_N}$ was then calculated by $\overline{\delta_N} = 2m\overline{C} + b$, where the overbar represents daytime averaging over 10 days in each period.

were greatly reduced under drought conditions, they recovered very quickly after rainfall. Although C_4 grasses have a higher intrinsic water use efficiency, their shallower effective rooting biomass becomes a greater constraint depressing the rate of photosynthesis under drought conditions.

[40] Having validated our modeling approach with two independent methods, we have confidence using modeled C_i/C_a and relative C_3/C_4 productivity to estimate bulk canopy discrimination (Δ_E), which is essential to partitioning NEE into its F_A and F_R components.

4.3. Partitioning NEE Into F_A and F_R

[41] Using equations (1) and (2) to partition NEE into photosynthesis and respiration will only work when isotope measurements provide additional information for labeling associated fluxes. At times when the difference between isotope ratios associated with each one-way flux is small, F_A and F_R cannot be discerned, i.e., $\delta_R = \delta_p (= \delta_N)$ and the ecosystem fluxes reach an "isotopic equilibrium." Under such conditions, stable isotope analyses of CO_2 do not provide any new information on CO_2 flux exchange rates and equations (1) and (2) converge into a single equation, eliminating the potential that stable isotope analyses of CO_2 can be used to separate NEE into F_A and F_R. This turns out to be the case for the drought period. Our estimate of mean $\delta_N = -15.4‰$ (described below) is very similar to the mean value of δ_R ($= -15.0‰$) under drought. For the wet period, $\delta_R = -12.1‰$ and this value is sufficiently different from the mean δ_N ($= -16.3‰$) to allow partitioning of NEE into its flux components. We therefore partitioned NEE into F_A and F_R only for the wet period.

[42] For the estimates of δ_N, δ_R, and δ_p, we used Keeling plot approach to measure δ_R and modeled δ_p by equations (7) and (8) after validating our process-based model with two independent methods. The largest uncertainty resides on the estimate of δ_N. A unique relationship between CO_2 and ^{13}C does not always exist in C_3-C_4 mixture grassland because of the distinct differences between C_3 and C_4 discrimination and how their relative contributions would affect any mixing curve. During the day, the isotopic heterogeneity effect is enhanced, partly caused by the dynamics of stomatal behavior and C_i. Characterizing δ_N can become very challenging in a heterogeneous ecosystem with more than one photosynthetic pathway. Figure 6 shows the relationship between daytime $\delta^{13}C$ and CO_2 concentration of flasked air samples for the dry period. Only flasks collected at the same height as the eddy covariance system were used. In order to obtain a significant range of CO_2 concentrations during periods of carbon uptake, flasks were collected every 2–3 hours from early morning until sunset for 3 consecutive days. During the drought period, we observed an 18 ppm range in CO_2 concentrations. The relationship between measured $\delta^{13}C$ and CO_2 concentration was significant ($R^2 = 0.38$). The regression coefficients were $m = -0.0228$ (±0.0051 SE) and $b = 0.1278$ (±1.9078 SE).

[43] This observed relationship represented an integrated daytime average because we used flasks collected over

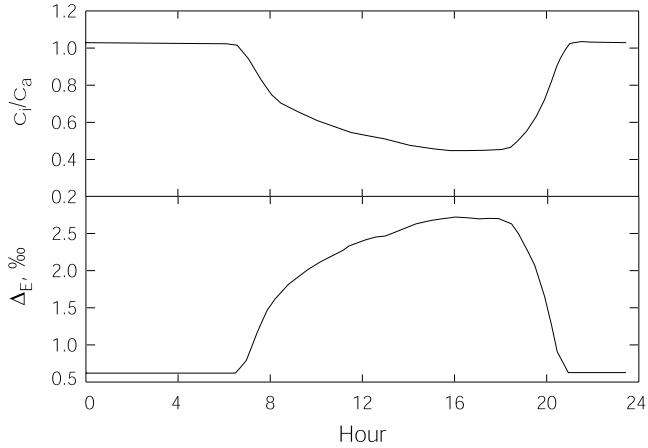

Figure 7. Modeled intercellular (C_i) to ambient (C_a) CO_2 concentration ratio and bulk canopy discrimination against ^{13}C during photosynthesis (Δ_E) for the wet period.

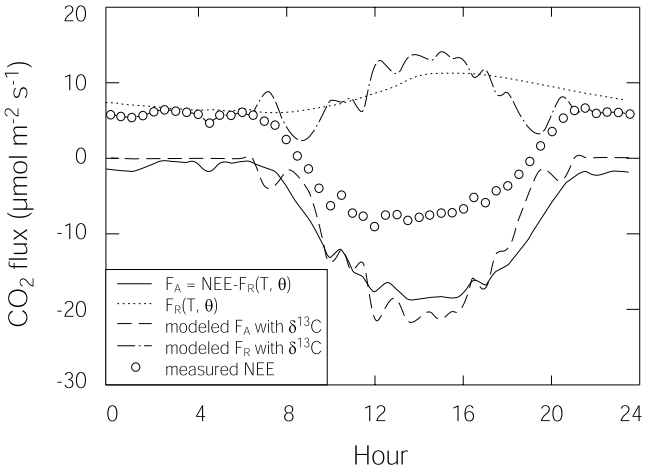

Figure 8. Partitioning of NEE measurements into photosynthesis (F_A) and respiration (F_R) components in a C_3-C_4 tallgrass prairie. Diurnal patterns of modeled F_A and F_R with a $\delta^{13}C$ approach are shown, along with chamber-based respiration estimates $F_R(T, \theta)$ and derived F_A, calculated as $F_A = \text{NEE} - R(T, \theta)$.

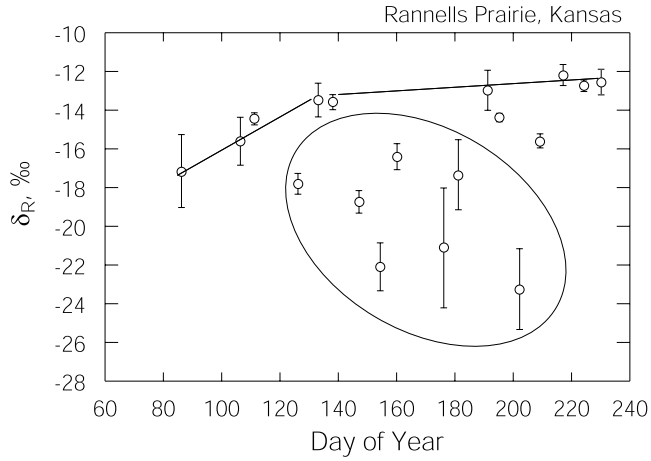

Figure 9. Carbon isotope ratios of ecosystem respiration (δ_R) measured at Rannells Flint Hills Prairie, Kansas, for the 2002 growing season. Values of δ_R are reported as means ±1 SE. Seasonal trends for the δ_R values are indicated by a solid line; δ_R values that are potentially reflecting surrounding C_3 sources are circled.

many hours, including early morning and late afternoon hours when atmospheric stability was in transition. During these transition periods, the turbulent transport became less stationary. Relationships between scalars and their source densities would likely be different from those observed during midday hours. The measured relationship between $\delta^{13}C$ and CO_2 concentration likely represented midday hours more reasonably because more flasks were collected during that period. When flasks collected in the transition period were eliminated from the regression analysis, a stronger linear relationship was obtained ($R^2 = 0.57$). The statistical power was inherently limited by the small range of CO_2 concentration encountered. In order to apply these regression results to partition NEE over a 24-hour cycle, we decided to retain flasks collected during the transition period for the rest of the analyses.

[44] We estimated mean $\delta_N (= 2m\overline{C} + b)$ for the two periods using the regression coefficients obtained above and the mean daytime CO_2 concentration averaged over 10 days for each of the two periods. The mean δ_N equals to −15.4 and −16.3‰ for the drought and the well-watered period, respectively. We assumed that the relationship between daytime $\delta^{13}C$ and CO_2 concentration did not significantly change after the rain, which permitted us to apply the regression results for the wet period. In applying equations (1) and (2), δ_N was computed using 30-min averaged CO_2 concentration.

[45] Figure 7 shows the modeled C_i/C_a and Δ for the wet period. The C_i/C_a ratio progressively decreased during the day to a minimum of 0.42 by late afternoon. With stomata open for carbon uptake during the morning optimal hours, C_i/C_a ratio was closer to unity. As air temperature gradually increased and vpd became greater, it is likely that the stomata partially closed and C_i/C_a decreased. Canopy discrimination inversely followed the pattern of C_i/C_a, increasing as the day progressed to a maximum value of 2.8‰.

Table 3. Regression Statistics for the Comparison Between Isotopically Modeled and Chamber-Measured F_A and F_R During the Wet Period[a]

Variables	A	B	R^2	RMSE	Difference in Daily Sum
F_A	0.85	−1.68	0.93	2.25	+30.9
F_R	0.39	5.09	0.45	2.25	−30.9

[a]The linear regression model is $y = Ax + B$, where y and x are measured and modeled variables, respectively. The statistical variables A and B represent the regression slope and intercept, respectively. The coefficient of determination (R^2) and the root-mean-square error (RMSE, μmol m^{-2} s^{-1}) are also shown. Differences in daily sum (μmol m^{-2} s^{-1}) for F_A and F_R are calculated as $\sum F_{\text{modeled}} - \sum F_{\text{measured}}$.

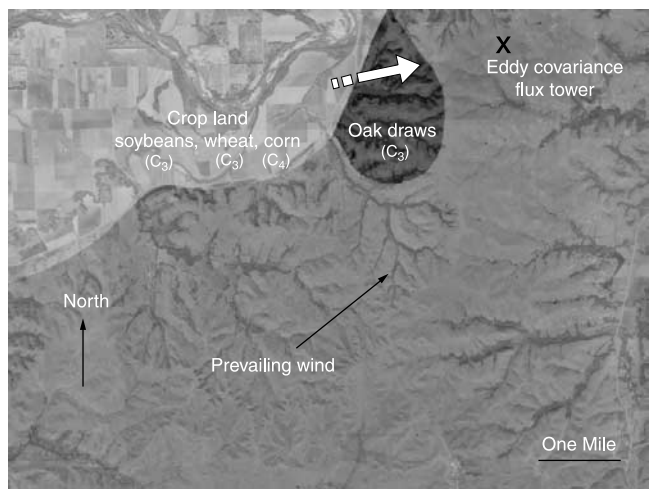

Figure 10. Map of land use for the surrounding area adjacent to our experimental C_4 prairie (unmarked area). Many C_3 sources are presented, including cropland (light area) and an oak forest (dark area). The location of the instrument tower is marked with a cross. The arrow indicates major wind directions when C_3-like isotopic signals are detected.

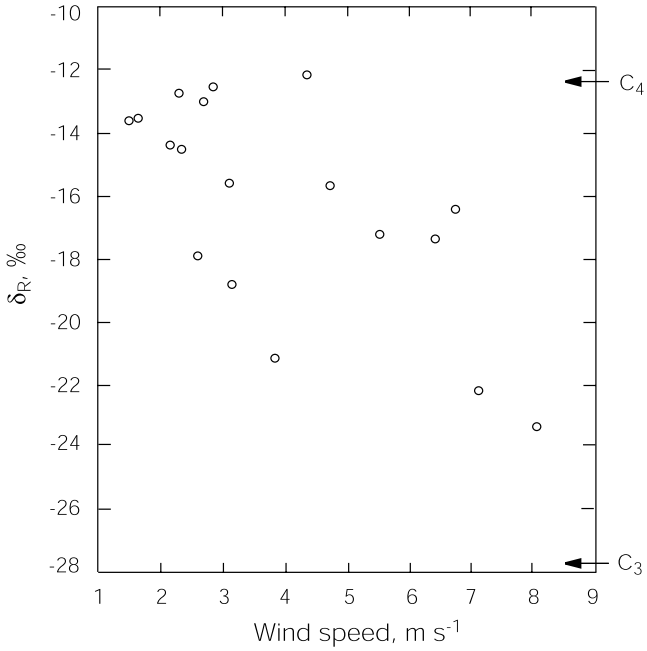

Figure 11. Relationships between observed δ_R values and the mean wind speed during the flask collection period.

This value was lower than the discrimination estimated from organic matter (4.3‰), which represented a long-term integrated value. The differences between long-term and instantaneous Δ were also addressed by *Farquhar et al.* [1989] and *Flanagan et al.* [1996], and there is no reason to expect that the short-term and long-term estimates of Δ values should always remain the same.

[46] With δ_N, δ_R, and δ_p values all measured or modeled, we partitioned NEE into F_A and F_R. Figure 8 shows the averaged diurnal pattern of modeled F_A and F_R values. The chamber-measured F_R and F_A (calculated as the difference between NEE and measured F_R) are also shown. The isotopic approach agreed reasonably well with chamber-based measurements during midday hours. Some differences were apparent in the early morning and later afternoon hours, possibly due to the collapse of the empirical relationship between $\delta^{13}C$ and CO_2 in these hours. While the diurnal patterns of F_A and F_R between the isotopically modeled and chamber-measured values are similar (Figure 8), the isotopic approach was more sensitive to temporal changes in F_A and F_R, perhaps due to isoflux dynamics in this ecosystem. The two approaches resulted in only a 10% difference in the daily sum of one-way gross fluxes (Table 3).

[47] An isotopic disequilibrium between photosynthetic and respiratory fluxes is required to use $\delta^{13}C$ for partitioning NEE. Seasonal and interannual variations in photosynthetic uptake have been observed for tallgrass ecosystems [*Ham and Knapp*, 1998; *Suyker and Verma*, 2001], thus discrimination values should vary as well. Such photosynthetic differences are also likely occurring at hourly timescales because of the sensitive stomatal responses to environmental perturbations [*Buchmann et al.*, 1996; *Long*, 1999].

5. Discussion

[48] We have shown that carbon isotope values of atmospheric CO_2 are useful tracers to partition the photosynthetic and respiratory fluxes contributing to net ecosystem exchange fluxes within a C_3-C_4 mixture grassland. The distinct differences between C_3 and C_4 carbon isotope discrimination provide different atmospheric imprints than would be expected for an ecosystem with only C_3 or only C_4 components. However, uncertainties in the atmospheric footprint sampled may obscure our understanding of using these techniques. We use our season-long δ_R measurements to illustrate one potential obstacle of isotopic air sampling in a tallgrass prairie surrounded by a different vegetation type and explain how atmospheric isotope measurements may provide additional information for assessing the fetch at eddy covariance stations in heterogeneous ecosystems.

[49] The weekly δ_R measurements for the entire growing season in 2002 are shown in Figure 9. The observed δ_R values were more negative in the early spring because of the higher percentage of active C_3 plants in this prairie. As the growing season progressed, δ_R became more ^{13}C enriched, reflecting the emerging dominance of C_4 species in primary productivity. Nonetheless, the C_3-to-C_4 seasonal pattern of δ_R values was obscured by occasional dramatic shifts between a C_3- and C_4-dominated signal from one week to another. After examining agricultural land use activities in the surrounding areas, we realized that our C_4 prairie was surrounded by several C_3 sources, both crops and forests

Table 4. Seasonal Variation in the Proportions of C_4 Photosynthesis at the Rannells Flint Hills Prairie in 2002[a]

DOY	δ_R, ‰	Standard Error, ‰	Wind Speed, m/s	Wind Direction, deg	C_4 (±SE), %
86	−17.2	1.91	5.54	291	68.5 (±12.2)
106	−15.7	1.26	4.73	195	78.5 (±8.1)
111	−14.5	0.31	2.34	115	86.1 (±2.0)
133	−13.5	0.87	1.65	297	92.4 (±5.6)
138	−13.6	0.39	1.51	62	91.8 (±2.5)
191	−13.0	1.07	2.70	111	95.8 (±6.9)
195	−14.4	0.23	2.16	47	86.9 (±1.5)
209	−15.6	0.35	3.11	272	79.0 (±2.2)
217	−12.1	0.56	4.36	24	100.0 (±3.6)
224	−12.7	0.29	2.30	110	97.4 (±1.9)
230	−12.5	0.67	2.85	46	98.7 (±4.3)

[a]The C_4 proportions were estimated by a two-end-member mixing model with $\delta^{13}C_3 = -27.9$ (±0.54 SE)‰ and $\delta^{13}C_4 = -12.3$ (±0.19 SE)‰. The wind speed and wind direction are the mean values averaged over the duration of flask collection. The wind direction is in degrees relative to the north counterclockwise.

(Figure 10). When δ_R values were plotted against the mean wind speed at the time of flask collection, we observed a pattern. As wind speed increased and increased the effective fetch distance, the measured isotopic signals of ecosystem respiration became more C_3-like, suggesting an input from the surrounding C_3 vegetation (Figure 11). A further analysis on the wind direction data showed that when the wind was blowing from WSW (between 110° and 130° counterclockwise), more C_3-like signals were observed, consistent with an expected impact from adjacent C_3 crops and forests. One implication is then that isotopic CO_2 sampling can be useful when evaluating the fetch of upwind airflow across a heterogeneous landscape, providing further information useful for interpreting eddy covariance observations.

[50] Excluding only δ_R values that were potentially reflecting surrounding C_3 sources (points that were circled in Figure 9), we calculated that the percentage of C_4 photosynthesis contributing to primary productivity for this tallgrass prairie ecosystem during the 2002 growing season increased from 68% in the early spring to nearly 100% in the late summer (Table 4). This change in the seasonal contribution of C_4 photosynthesis to primary productivity is in agreement with a similar C_3-C_4 prairie in north central Oklahoma [*Still et al.*, 2003].

6. Conclusions

[51] Carbon isotope measurements are useful to distinguish the contributions of C_3 and C_4 photosynthesis to net ecosystem CO_2 exchange fluxes and also to partition NEE into photosynthetic and respiratory components in a tallgrass prairie. The proportion of C_4 photosynthesis increased from 68% to nearly 100% between early spring and late summer as air temperature increased. Partitioning NEE into its photosynthesis and respiration components using $\delta^{13}C$ of atmospheric CO_2 requires an isotopic disequilibrium between photosynthetic and respiratory fluxes. Season-long δ_R measurements showed large isotopic fluctuations reflecting temporal differences in the C_3/C_4 contributions to NEE. Further analyses of δ_R values indicated that adjacent C_3 ecosystems could be detected under appropriately high wind speed and wind direction conditions.

Notation

A_0 leaf photosynthetic rate at the top of the canopy, μmol m^{-2} s^{-1}.
A_n net photosynthetic rate, μmol m^{-2} s^{-1}.
a diffusional fractionation factor, ‰.
b intercept of a linear regression between $\delta^{13}C_a$ and CO_2 concentration.
b_x enzymatic fractionation factor, ‰.
b_s stomatal intercept parameter.
C CO_2 concentration, μmol mol^{-1}.
$\overline{C}$ time-averaged CO_2 concentration, μmol mol^{-1}.
C_a atmospheric CO_2 concentration, μmol mol^{-1}.
C_i bulk canopy intercellular CO_2 concentration, μmol mol^{-1}.
C_s CO_2 concentration at the leaf surface, μmol mol^{-1}.
F_A canopy photosynthetic flux density, μmol m^{-2} s^{-1}.
F_R ecosystem respiratory flux density, μmol m^{-2} s^{-1}.
F_δ isoflux, μmol m^{-2} s^{-1} ‰.
f fraction of C_4 contribution to canopy assimilation.
f_w water stress factor.
G_c bulk canopy conductance, mol m^{-2} s^{-1}.
g_s stomatal conductance, mol m^{-2} s^{-1}.
h canopy height, m.
J_C Rubisco-limited assimilation rate, μmol m^{-2} s^{-1}.
J_E light-limited assimilation rate, μmol m^{-2} s^{-1}.
J_S sucrose-export limited assimilation rate, μmol m^{-2} s^{-1}.
$\overline{k}$ time-averaged canopy extinction coefficient.
LAI total leaf area index, m^2 m^{-2}.
L_T leaf area index for C_3 or C_4, m^2 m^{-2}.
m slope of a linear regression between $\delta^{13}C_a$ and CO_2 concentration.
m_s stomatal slope parameter.
NEE net ecosystem exchange for CO_2 fluxes, μmol m^{-2} s^{-1}.
Q_p photosynthetic photon flux density, μmol m^{-2} s^{-1}.
R molar ratio of heavy to light isotope ($^{13}C/^{12}C$).
R_d dark respiration rate, μmol m^{-2} s^{-1}.
RH relative humidity.
R_{soil} rate of soil respiration, g C m^{-2} d^{-1}.
R_{std} molar ratio of heavy to light isotope for a known standard.
T_a air temperature, °C.
T_l leaf surface temperature, °C.
T_s soil temperature, °C.
V_{cmax} maximum Rubisco capacity at 25°C, μmol m^{-2} s^{-1}.
V_m Rubisco capacity, μmol m^{-2} s^{-1}.
vpd vapor pressure deficit, kPa.
w vertical wind speed, m s^{-1}.
ρ air density, mol m^{-3}.
v canopy greenness fraction.
λ clumping factor.
Π scaling factor.
θ surface soil moisture content, m^3 m^{-3}.
$\delta^{13}C$ carbon isotopic composition, ‰.
$\delta^{13}C_3$ carbon isotopic composition of C_3 organic matter, ‰.
$\delta^{13}C_4$ carbon isotopic composition of C_4 organic matter, ‰.
$\delta^{13}C_a$ $\delta^{13}C$ of canopy air, ‰.
$\delta^{18}O$ oxygen isotopic composition, ‰.
δ_p isotopic composition of the CO_2 assimilated via photosynthesis, ‰.
δ_a $\delta^{13}C$ of background CO_2, ‰.
θi soil moisture content at the onset of water stress, m^3 m^{-3}.
δ_N isotopic composition of CO_2 associated with NEE exchange, ‰.
δ_R isotopic composition of ecosystem respired CO_2, ‰.
θ_w soil moisture content at wilting point m^3 m^{-3}.
Δ discrimination against ^{13}C during photosynthesis, ‰.
Δ_E canopy-scale discrimination, ‰.

[52] **Acknowledgments.** This study was supported by the Department of Energy, through the Terrestrial Carbon Processes (TCP) Project under agreement DE-FG03-00ER63012. The authors thank Dave Bowling for useful discussions on NEE partitioning and comments on the manuscript. Joe Berry provided helpful discussions on the effect of soil moisture on Rubisco capacity in the photosynthesis model. The authors also thank

Lisa Auen, Erik Stange, and Timothy Jackson for field assistance and laboratory sample preparation. Craig Cook, Mike Lott, and Big Dog provided excellent assistance with isotopic analyses.

References

Axmann, B. D., and A. K. Knapp, Water relations of *Juniperus virginiana* and *Andropogon gerardii* in an unburned tallgrass prairie watershed, *Southwest. Nat.*, *38*, 325–330, 1993.

Baldocchi, D. D., and D. R. Bowling, Modeling the discrimination of $^{13}CO_2$ above and within a temperate broad-leaved forest canopy on hourly to seasonal time scales, *Plant Cell Environ.*, *26*, 231–244, 2003.

Ball, J. T., I. E. Woodrow, and J. A. Berry, A model predicting stomatal conductance and its contribution to the control of photosynthesis under different environmental conditions, in *Progress in Photosynthesis Research*, vol. 4, edited by I. Biggins, pp. 221–224, Martinus Nijhoff, Zoetermeer, Netherlands, 1987.

Bowling, D. R., D. D. Baldocchi, and R. K. Monson, Dynamics of isotopic exchange of carbon dioxide in a Tennessee deciduous forest, *Global Biogeochem. Cycles*, *13*(4), 903–922, 1999.

Bowling, D. R., P. P. Tans, and R. K. Monson, Partitioning net ecosystem carbon exchange with isotopic fluxes of CO_2, *Global Change Biol.*, *7*, 127–145, 2001a.

Bowling, D. R., C. S. Cook, and J. R. Ehleringer, Technique to measure CO_2 mixing ratio in small flasks with a bellows/IRGA system, *Agric. For. Meteorol.*, *109*, 61–65, 2001b.

Bowling, D. R., N. G. McDowell, B. J. Bond, B. E. Law, and J. R. Ehleringer, ^{13}C content of ecosystem respiration is linked to precipitation and vapor pressure deficit, *Oecologia*, *131*, 113–124, 2002.

Bowling, D. R., D. E. Pataki, and J. R. Ehleringer, Critical evaluation of micrometeorological methods for measuring ecosystem-atmosphere isotopic exchange of CO_2, *Agric. For. Meteorol.*, *116*, 159–179, 2003.

Buchmann, N., J. R. Brooks, K. D. Rapp, and J. R. Ehleringer, Carbon isotope composition of C_4 grasses is influenced by light and water supply, *Plant Cell Environ.*, *19*, 392–402, 1996.

Campbell, G. S., and J. M. Norman, *An Introduction to Environmental Biophysics*, 240 pp., Springer-Verlag, New York, 1998.

Campbell, G. S., C. Calissendorf, and J. H. Williams, Probe for measuring soil specific heat using a heat pulse method, *Soil Sci. Soc. Am. J.*, *55*, 291–293, 1991.

Chen, D.-X., M. B. Coughenour, A. K. Knapp, and C. E. Owensby, Mathematical simulation of C_4 grass photosynthesis in ambient and elevated CO_2, *Ecol. Modell.*, *73*, 63–80, 1994.

Ciais, P., P. P. Tans, M. Trolier, J. W. C. White, and R. J. Francey, A large Northern Hemisphere terrestrial CO_2 sink indicated by the $^{13}C/^{12}C$ ratio of atmospheric CO_2, *Science*, *269*, 1098–1102, 1995.

Colello, G. D., V. Grivet, P. J. Sellers, and J. A. Berry, Modeling of energy, water, and CO_2 flux in a temperate grassland ecosystem with SiB2: May–October 1987, *J. Atmos. Sci.*, *55*, 1141–1169, 1998.

Collatz, G. J., M. Ribas-Carbo, and J. A. Berry, Coupled photosynthesis-stomatal conductance model for leaves of C_4 plants, *Aust. J. Plant Physiol.*, *19*, 519–538, 1992.

Ehleringer, J. R., and C. S. Cook, Carbon and oxygen isotope ratios of ecosystem respiration along an Oregon conifer transect: Preliminary observations based on small-flask sampling, *Tree Physiol.*, *18*, 513–519, 1998.

Farquhar, G. D., and J. Lloyd, Carbon and oxygen isotope effects in the exchange of carbon dioxide between terrestrial plants and the atmosphere, in *Stable Isotopes and Plant Carbon-Water Relations*, edited by J. R. Ehleringer, A. E. Hall, and G. D. Farquhar, pp. 47–70, Academic, San Diego, Calif., 1993.

Farquhar, G. D., S. Von Caemmerer, and J. A. Berry, A biochemical model of photosynthetic CO_2 assimilation in leaves of C_3 species, *Planta*, *149*, 78–90, 1980.

Farquhar, G. D., J. R. Ehleringer, and K. T. Hubick, Carbon isotope discrimination and photosynthesis, *Annu. Rev. Plant Physiol. Plant Mol. Biol.*, *40*, 503–537, 1989.

Field, C. B., Ecological scaling of carbon gain to stress and resource availability, in *Response of Plants to Multiple Stresses*, edited by H. A. Mooney, W. E. Winner, and E. J. Pell, pp. 35–65, Academic, San Diego, Calif., 1991.

Flanagan, L. B., and J. R. Ehleringer, Ecosystem-atmosphere CO_2 exchange: Interpreting signals of change using stable isotope ratios, *Trends Ecol. Evol.*, *13*(1), 10–14, 1998.

Flanagan, L. B., J. R. Brooks, G. T. Varney, S. C. Berry, and J. R. Ehleringer, Carbon isotope discrimination during photosynthesis and the isotope ratio of respired CO_2 in boreal forest ecosystems, *Global Biogeochem. Cycles*, *10*(4), 629–640, 1996.

Francey, R. J., P. P. Tans, and C. E. Allison, Changes in oceanic and terrestrial carbon uptake since 1982, *Nature*, *373*, 326–330, 1995.

Goulden, M. L., J. W. Munger, S.-M. Fan, B. C. Daube, and S. C. Wofsy, Measurements of carbon sequestration by long-term eddy covariance: Methods and a critical evaluation of accuracy, *Global Change Biol.*, *2*, 169–182, 1996.

Ham, J. M., and J. L. Heilman, Experimental test of density and energy-balance corrections on CO_2 flux as measured using open-path eddy covariance, *Agron. J.*, in press, 2003.

Ham, J. M., and A. K. Knapp, Fluxes of CO_2, water vapor, and energy from a prairie ecosystem during the seasonal transition from carbon sink to carbon source, *Agric. For. Meteorol.*, *89*, 1–14, 1998.

Hirose, T., and M. J. A. Werger, Maximizing daily canopy photosynthesis with respect to the leaf nitrogen allocation pattern in the canopy, *Oecologia*, *72*, 520–526, 1987.

Keeling, C. D., The concentrations and isotopic abundances of atmospheric carbon dioxide in rural areas, *Geochim. Cosmochim. Acta*, *13*, 322–334, 1958.

Keeling, C. D., W. G. Mook, and P. P. Tans, Recent trends in the $^{13}C/^{12}C$ ratio of atmospheric carbon dioxide, *Nature*, *277*, 121–123, 1979.

Keeling, C. D., T. P. Whorf, M. Wahlen, and J. van der Plicht, Interannual extremes in the rate of rise of atmospheric carbon dioxide since 1980, *Nature*, *375*, 666–670, 1995.

Kim, J., and S. B. Verma, Modeling canopy stomatal conductance in a temperate grassland ecosystem, *Agric. For. Meteorol.*, *55*, 149–166, 1991.

Kim, J., S. B. Verma, and R. J. Clement, Carbon dioxide budget in temperate grassland ecosystem, *J. Geophys. Res.*, *97*, 6057–6063, 1992.

Knapp, A. K., Post-fire water relations, production and biomass allocation in the shrub, *Rhus glabra*, in tallgrass prairie, *Botan. Gaz.*, *147*, 90–97, 1986.

Knapp, A. K., and E. Medina, Success of C_4 photosynthesis in the field: Lessons from communities dominated by C_4 plants, in *C_4 Plant Biology*, edited by R. F. Sage and R. F. Monson, pp. 251–283, Academic, San Diego, Calif., 1999.

Knapp, A. K., and T. R. Seastadt, Grassland, konza prairie, and long-term ecological research, in *Grassland Dynamics: Long-Term Ecological Research in Tallgrass Prairie*, edited by A. K. Knapp et al., pp. 3–15, Oxford Univ. Press, New York, 1998.

Lai, C.-T., G. G. Katul, R. Oren, D. Ellsworth, and K. Schäfer, Modeling CO_2 and water vapor turbulent flux distributions within a forest canopy, *J. Geophys. Res.*, *105*, 26,333–26,351, 2000.

Lai, C.-T., G. Katul, J. Butnor, D. Ellsworth, and R. Oren, Modelling nighttime ecosystem respiration by a constrained source optimization method, *Global Change Biol.*, *8*, 124–141, 2002a.

Lai, C.-T., G. G. Katul, J. Butnor, M. Siqueira, D. Ellsworth, C. Maier, K. Johnsen, S. Mckeand, and R. Oren, Modelling the limits on the response of net carbon exchange to fertilization in a south-eastern pine forest, *Plant Cell Environ.*, *25*, 1095–1119, 2002b.

Lavigne, M. B., et al., Comparing nocturnal eddy covariance measurements to estimates of ecosystem respiration made by scaling chamber measurements at six coniferous boreal sites, *J. Geophys. Res.*, *102*, 28,977–28,985, 1997.

Leuning, R., F. M. Kelliher, D. G. G. De Pury, and E.-D. Schulze, Leaf nitrogen, photosynthesis, conductance and transpiration: Scaling from leaves to canopies, *Plant Cell Environ.*, *18*, 1183–1200, 1995.

Lin, G., and J. R. Ehleringer, Carbon isotopic fractionation does not occur during dark respiration in C_3 and C_4 plants, *Plant Physiol.*, *114*, 391–394, 1997.

Lloyd, J., and G. D. Farquhar, ^{13}C discrimination during CO_2 assimilation by the terrestrial biosphere, *Oecologia*, *99*, 201–215, 1994.

Long, S. P., Environmental responses, in *C_4Plant Biology*, edited by R. F. Sage and R. F. Monson, pp. 251–283, Academic, San Diego, Calif., 1999.

Mielnick, P. C., and W. A. Dugas, Soil CO_2 flux in a tallgrass prairie, *Soil Biol. Biochem.*, *32*, 221–228, 2000.

Mook, W. G., M. Koopmans, A. F. Carter, and C. D. Keeling, Seasonal, latitudinal, and secular variations in the abundance and isotopic-ratios of atmospheric carbon-dioxide: 1. Results from land stations, *J. Geophys. Res.*, *88*, 915–933, 1983.

Pataki, D. E., J. R. Ehleringer, L. B. Flanagan, D. Yakir, D. R. Bowling, C. J. Still, N. Buchmann, J. O. Kaplan, and J. A. Berry, The application and interpretation of Keeling plots in terrestrial carbon cycle research, *Global Biogeochem. Cycles*, *17*(1), 1022, doi:10.1029/2001GB001850, 2003.

Raupach, M. R., Inferring biogeochemical sources and sinks from atmospheric concentrations: General consideration and application in vegetation canopies, in *Global Biogeochemical Cycles in the Climate System*, edited by E. D. Schulze et al., pp. 41–60, Academic, San Diego, Calif., 2001.

Schauer, A. J., C.-T. Lai, D. R. Bowling, and J. R. Ehleringer, An automated sampler for collection of atmospheric trace gas samples for stable isotope analyses, *Agric. For. Meteorol.*, *118*, 113–124, 2003.

Sellers, P. J., Canopy reflectance, photosynthesis and transpiration, *Int. J. Remote Sens.*, *8*, 1335–1372, 1985.

Sellers, P. J., et al., A revised land surface parameterization (SiB2) for atmospheric GCMs, part I. Model formulation, *J. Clim.*, *9*, 676–705, 1996.

Sokal, R. R., and F. J. Rohlf, *Biometry: The Principles and Practice of Statistics in Biological Research*, W. H. Freeman, New York, 1995.

Steward, J. B., and S. B. Verma, Comparison of surface fluxes and conductances at two contrasting sites within the FIFE area, *J. Geophys. Res.*, *97*, 18,623–18,628, 1992.

Still, C. J., J. A. Berry, M. Ribas-Carbo, and B. R. Helliker, The contribution of C_3 and C_4 plants to the carbon cycle of a tallgrass prairie: An isotopic approach, *Oecologia*, in press, 2003.

Suyker, A. E., and S. B. Verma, Year-round observations of the net ecosystem exchange of carbon dioxide in a native tallgrass prairie, *Global Change Biol.*, *7*, 279–289, 2001.

Tans, P. P., J. A. Berry, and R. F. Keeling, Oceanic $^{13}C/^{12}C$ observations: A new window on ocean CO_2 uptake, *Global Biogeochem. Cycles*, *7*(2), 353–368, 1993.

Tarara, J. M., and J. M. Ham, Measuring soil water content in the laboratory and in the field with dual probe heat capacity sensors, *Agron. J.*, *89*, 535–542, 1997.

Verma, S. B., J. Kim, and R. J. Clement, Momentum, water vapor, and carbon dioxide exchange at a centrally located prairie site during FIFE, *J. Geophys. Res.*, *97*, 18,629–18,640, 1992.

Weaver, J. E., Classification of root systems of forbs of grassland and a consideration of their significance, *Ecology*, *39*, 393–401, 1958.

Webb, E. K., G. I. Pearman, and R. Leuning, Correction of flux measurements for density effects due to heat and water vapour transfer, *Q. J. R. Meteorol. Soc.*, *106*, 85–100, 1980.

Yakir, D., and S. L. Sternberg, The use of stable isotopes to study ecosystem gas exchange, *Oecologia*, *123*, 297–311, 2000.

Yakir, D., and X.-F. Wang, Fluxes of CO_2 and water between terrestrial vegetation and the atmosphere estimated from isotope measurements, *Nature*, *380*, 515–517, 1996.

J. R. Ehleringer, C.-T. Lai, and A. J. Schauer, Department of Biology, University of Utah, 257 South 1400 East, Salt Lake City, UT 84112-0820, USA. (ehleringer@biology.utah.edu; lai@biology.utah.edu; schauer@biology.utah.edu)

J. M. Ham and C. Owensby, Department of Agronomy, Kansas State University, Manhattan, KS 66506, USA. (snafu@ksu.edu; owensby@ksu.edu)